Taylor & Francis
Taylor & Francis Group

Automatika

Journal for Control, Measurement, Electronics, Computing and Communications

ISSN: 0005-1144 (Print) 1848-3380 (Online) Journal homepage: http://www.tandfonline.com/loi/taut20

Analysis of electric field and emission spectrum in the glow discharge of therapeutic plasma electrode

D. Prebeg, B. Pavelić, M. Cifrek, S. Milošević, I. Krois, S. Šegović, M. Katunaruć & M. Kordić

To cite this article: D. Prebeg, B. Pavelić, M. Cifrek, S. Milošević, I. Krois, S. Šegović, M. Katunaruć & M. Kordić (2017) Analysis of electric field and emission spectrum in the glow discharge of therapeutic plasma electrode, Automatika, 58:1, 1-10, DOI: 10.1080/00051144.2017.1293921

To link to this article: https://doi.org/10.1080/00051144.2017.1293921

Published online: 06 Mar 2017.

AUTOMATIKA, 2017
VOL. 58, NO. 1, 1–10
http://dx.doi.org/10.1080/00051144.2017.1293921

Taylor & Francis
Taylor & Francis Group

REGULAR PAPER

OPEN ACCESS

Analysis of electric field and emission spectrum in the glow discharge of therapeutic plasma electrode

D. Prebeg[a], B. Pavelić[a], M. Cifrek[b], S. Milošević[c], I. Krois[d], S. Šegović[a], M. Katunarić[a] and M. Kordić[e]

[a]Department of Endodontics and Restorative Dentistry, School of Dental Medicine, University of Zagreb, Zagreb, Croatia; [b]Faculty of Electrical Engineering and Computing, Department of Electronic Systems and Information Processing, University of Zagreb, Zagreb, Croatia; [c]Institute of Physics, Zagreb, Croatia; [d]Faculty of Electrical Engineering and Computing, Department for Electronics, Microelectronics, Computer and Intelligent Systems, University of Zagreb, Zagreb, Croatia; [e]Faculty of Electrical Engineering and Computing, Department of Electrical Engineering Fundamentals and Measurements, University of Zagreb, Zagreb, Croatia

ABSTRACT

Gas-filled glass plasma electrodes coupled with high-frequency high-voltage generators are used in medicine and dentistry for more than a century. In recent literature, therapeutic effects of such procedure have been explained through topical bio-oxidative effects of ozone generated by the dielectric barrier discharge. The aim of this study was to evaluate characteristics of electric field and optical emission spectrum generated in the treatment field by the glow discharge of the plasma electrode. Emission spectrum in red and near-infrared wavelength range (540–886 nm) and pulsed electric field (impulse frequency 1053 Hz, exponentially damped sine wave in the range of 33 kHz, duty cycle 20%) were recorded. Estimated electric field strength at 1-mm distance was in the range from 5.8 to 13.7 kV/m and between 10^6 and 10^8 V/m in the close proximity of electrode's surface (below 0.01 mm). Recorded factors are integral constituents in the treatment field and their properties can be correlated to the known biological and therapeutic effects of photostimulation and electrostimulation. These factors present important bioactive components which could be responsible for therapeutic effects, reported in number of clinical studies, especially those which could not be explained through topical bio-oxidative effects of ozone.

ARTICLE HISTORY
Received 2 December 2016
Accepted 17 January 2017

KEYWORDS
Electric field; emission spectrum; cold atmospheric plasma; glow discharge electrode

Introduction

Sir William Crookes discovered plasma in 1879 using electrical discharge tube with partial vacuum (Crooks tube) [1]. Plasma, the fourth and most abundant fundamental state of matter, is made up of unbound charged particles (electrons and ions) as well as photons, free radicals, metastable and neutral atoms and molecules [2]. It is characterized by collective behaviour of the particles due to the long-range electromagnetic (coulomb) forces, whereas the overall charge of plasma is roughly zero [3].

Plasmas are classified with respect to the relative temperature of their constituents as "thermal" and "non-thermal". In the thermal plasma all particles are at the same temperature, whereas in the non-thermal plasma ions and electrically neutral species are at a much lower temperature than electrons. A specific type of non-thermal plasma is cold atmospheric plasma (CAP) produced at atmospheric pressure and its temperature at the point of application is less than 40 °C [4]. Thanks to the low temperature and the possibility of its application on living tissue as well as the numerous bioactive properties of CAP, a whole new field of plasma medicine is established [5,6].

Plasma, excluding solid-state plasmas or phenomena like lightning and aurora, does not occur naturally at the surface of the Earth [3]. Hence for investigations of plasmas and their technological applications they must be produced artificially. Currently, substantial efforts are being made in plasma medicine to develop the best-suited plasma device for the given medical indication [4,6]. There are numerous device configurations, which differ in their geometry, number and location of electrodes, and the nature of initiating and sustaining electric or electromagnetic fields (EMFs), which have been recognized as the most suitable and cost-effective sources for the production of CAP [4].

CAP used for healthcare can be dated back as early as the middle of the nineteenth century [6]. CAP devices comprised gas-filled glass electrode (plasma electrode) coupled with high-frequency high-voltage source (namely *Tesla coil*) are applied in medicine for more than one century, and millions of treatments were performed through such method [7–9]. However, due to the lack of basic and practical research, their therapeutic applicability is still unrecognized by the scientific and medical community.

CONTACT D. Prebeg dprebeg@sfzg.hr

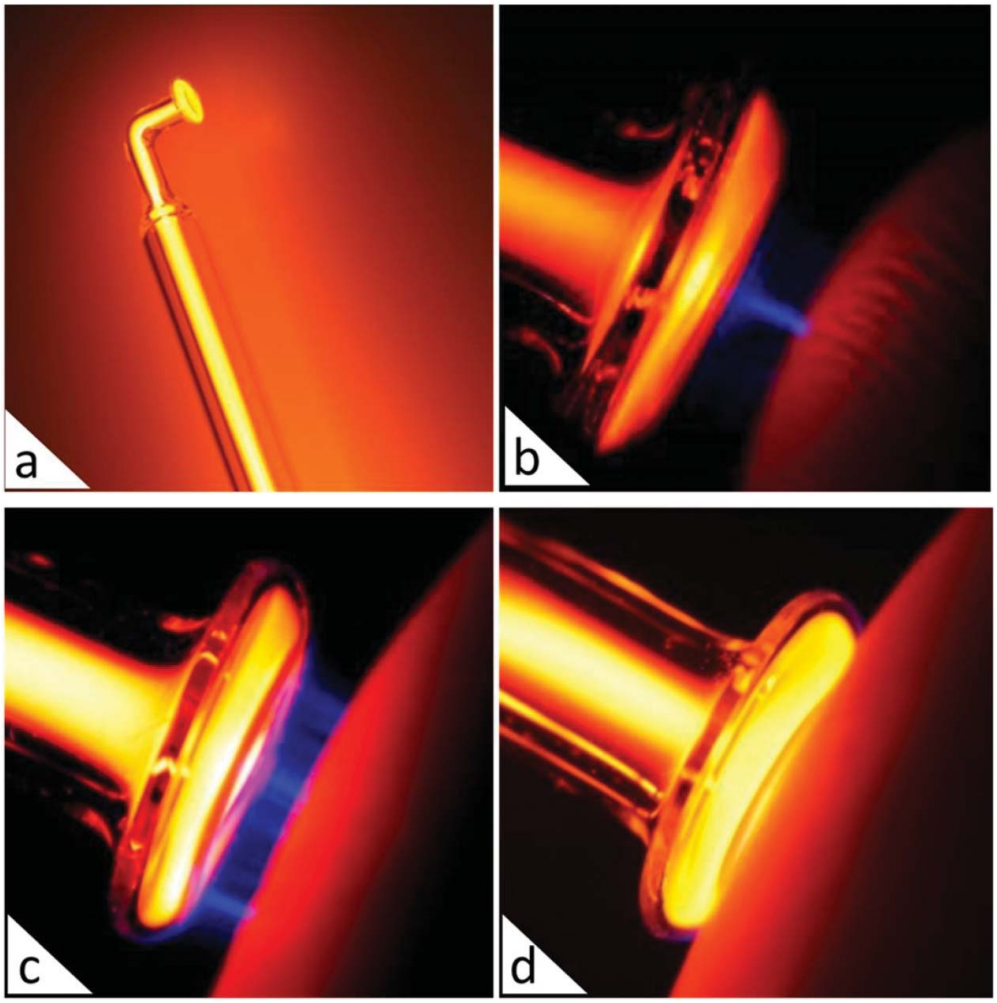

Figure 1. Glow discharge of the plasma electrode: (a) lens-shaped plasma electrode in standby mode (tenuous glow discharge inside the lumen of the glass tube); (b) initial DBD streamer is formed as the electrode approaches the surface of the skin (glow discharge is still tenuous); (c) developed DBD in the air gap as the distance between electrode and skin is reduced (intensified glow discharge); (d) plasma electrode in direct contact with skin (intensified glow discharge without visible DBD).

A plasma electrode is a sealed partially evacuated glass tube filled with air, noble gas or other gas mixtures in which high-voltage high-frequency oscillating current causes formation of, apparently homogeneous, diffuse discharges (Figure 1(a)) which are referred to as radio-frequency glow discharges [10]. For the purpose of the therapeutic procedure, plasma electrode is applied either directly to the patient skin and mucosa or is brought at distance of few millimetres from their surface (Figure 1(b–d)) [9]. In the later, generation of dielectric barrier discharge (DBD), which consists of numerous micro-discharges, is obtained in the air gap between the electrode and the treated surface. By applying a sufficient electric field, which is larger than the dielectric strength of the air (3×10^6 V/m) [11], a local breakdown is initiated in which growing electron avalanches quickly produce such a high space charge that self-propagating streamers are formed (Figure 1(b–c)) [10]. For more than a century, DBD is used for generation of ozone, but recently its ability to generate CAP has been recognized [12].

In recent years, therapeutic method using CAP devices comprised plasma electrode coupled with high-frequency, high-voltage source re-entered clinical application in medicine and dentistry. A clinical evaluation of such method indicates positive results in disinfection [13–15] post-surgical soft tissue and bone healing and pain relief [16–20], treatment of various oral and dental diseases [21–24], reduction of temporomandibular disorder-related pain [25], and bisphosphonate-related osteonecrosis of the jaw [26]. In recent available literature found on the clinical application of plasma electrode coupled with high-frequency generator, all of the reported therapeutic effects are generally ascribed to bio-oxidative effects of ozone [14-26].

When gaseous ozone is administered in the treatment field, e.g. using ozone-producing syringe as described in our recent paper [13], the therapeutic effects can indeed be ascribed exclusively to ozone [27]. Similarly, when ozone is produced through DBD and CAP generation, in the air gap between plasma electrode and treated surface as reported by Tuncer

et al. [14] or Wilczynska et al. [15], the positive therapeutic effects could be ascribed to a topical antiseptic and bio-simulative effects of both ozone and CAP [4]. Graves [28] gave detailed background on CAP's underlying therapeutic mechanisms emphasizing the role of reactive oxygen and nitrogen species as the most important therapeutic agents in the course of CAP treatment. However, in the treatment modes when plasma electrode is applied in direct contact with the treated surface (especially in treatment of tissues underlying intact skin) or is immersed in liquids (e.g. saliva or blood), in which DBD and ozone generation are limited or even missing (Figure 1(d)), therapeutic effects, like improved bone healing and pain reduction, are still observed [17–19,25].

Erdemci et al. [29], in the study in which they have used short-duration treatments with plasma electrode on the extraction wound (AL probe, 30 s, 80% output intensity, at days 0 and 2), presumed that preoperative topical application of ozone was too distant to affect the alveolus and during the postoperative period the presence of a clot in the socket may have prevented the ozone reaching and affecting the bony surfaces of the alveolus. On the other hand, Filipović et al. [16] reported the intensity of pain and other discomforts, after surgical extraction of the impacted third lower molar, were significantly more reduced in patients who received the "ozone" therapy through single postoperative treatment of an extraction wound with combined ozone gas (ozone-producing syringe, KP probe, for 40 s) and plasma electrode application (AL and GI probe, 40 s each, at 80% output intensity).

Furthermore, Kazancioglu et al. [17] reported that degree of pain and the number of analgesic tablets taken was significantly lower after extra-oral application of the plasma electrode at the insertion point of the masseter muscle after the third molar extraction (Omega probe, 80% intensity for 10 min on postoperative days 0, 1, 3, 5 and 7) but were not able to explain how ozone contributed to the regulation and/or inhibition of the transmission of the pain signal to the central nervous system. Kazancioglu et al. [18] also demonstrated that both plasma electrode (120 s, three times a week for two weeks) and laser treatments (808 nm; 0.1 W, 4 J/cm) had a positive effect on bone formation in rat calvarial defect.

Ozdemir et al. [19] reported results which demonstrate that application of plasma electrode (PA probe at 80% for 30 s, three times a week for two weeks) augments new bone formation and leads to a simultaneous amplification of osteoblasts after the bone graft surgery. Taşdemir et al. [20] reported plasma electrode application (CA probe for 30 s at 75% at days 0 and 1, and 30% at day 2 post-surgically), in early healing period of de-epithelialized gingival graft, enhanced blood perfusion units in the first postoperative week. They also reported improvement in wound healing accompanied by an increase in the quality of life and decrease in postoperative pain. Doğan et al. [25] reported application of the plasma electrode (Omega probe, for 10 min, three times in one week) applied to the skin in the projection of underlying temporomandibular joint (TMJ) to be more effective treatment than medication therapy for relieving TMJ-related pain.

In view of the above clinical reports [17–19,25], we propose a hypothesis that not only bio-oxidative effects of ozone but also the effects of emission spectrum and electric field, which are generated by the glow discharge of the plasma electrode (Figure 1), and therefore are present in the treatment field, have to be taken into consideration as bioactive components in course of such treatment. By our knowledge, there are no reports in the appropriate literature regarding the presence or quantification of the named factors in the treatment field during the procedure. Assuming that these factors could have significant role in the course of treatment, we conducted investigation with an aim to confirm their presence and evaluate their properties in the treatment field. We report results of the electric field and optical emission spectrum measurements of the plasma electrode's glow discharge and compare them, with respect to their properties, with biological and therapeutic effects of photostimulation and electrostimulation recognized by the relevant literature.

Table 1. Wavelengths of the most evident lines in the emission spectrum of the glow discharge of the recorded at distance of 60 mm from the lens-shaped part of the plasma electrode.

Spectrum of neutral neon atom (Ne I) (nm)					
540.06	602.99*	630.48	667.83*	743.89*	849.53
576.44	607.43*	632.82*	671.7*	748.89	859.12
585.24*	609.62*	633.44*	692.95*	753.57	863.46
588.19*	612.85	638.3*	702.41	754.40	865.43
590.64	614.31*	640.23*	703.24	793.69	878.06
594.48*	616.36*	650.65*	705.13	794.32	885.38
596.55	618.22	653.29*	705.91*	830.03	886.57
597.55	621.73	659.9*	717.39	837.76*	
598.79	626.65*	665.21	724.52*	841.84	
Spectrum of neutral oxygen atom (O I) (nm)					
700.23	777.54*	777.19*	844.63*		

*The most expressive lines.

Materials and methods

Investigated device

Ozonix generator (Biozonix GmbH, Munich, Germany) was used in investigations described in this paper. The used model consists of a central unit, a patient grounding, an applicator and different models of plasma electrodes designed for intra- and extra-oral application in dentistry (Figure 2). The lens-shaped plasma electrode having the diameter of 8 mm (GI probe, product number 1005, Biozonix GmbH, Munich, Germany) was selected and its glow discharge investigated (Figure 2). In the menu of the central unit, the output intensity from 10% to 100% (output voltage

Figure 2. Ozonix generator used in this investigation: (a) generator; (b) patient grounding electrode; (c) applicator; (d) glass plasma electrode (for application in dentistry different shapes of electrodes are available, e.g. GI, AL, CA, PA probe); (e) investigated lens-shaped plasma electrode (GI probe, product number 1005, diameter = 8 mm) recommended for disinfection and stimulation of soft tissues; (f) ozone-producing syringe (KP probe) recommended for installation of gaseous ozone in treatment of root canals and periodontal pockets; (g) double plasma electrode (Omega probe) recommended for extra-oral treatment of pain and TMD (data according to manufacturer Biozonix GmbH, Munich, Germany – image created by Domagoj Prebeg).

from 3 to 18 kV, according to manufacturer) was adjusted depending on the requirements of the investigation.

In order to differ the factors generated by the glow discharge of the plasma electrode from the factors generated by DBD, all measurements were carried out for the standby mode of the electrode (see Figure 1(a)). Thus, measurements were done at sufficient distances from lens-shaped surface of the electrode which precluded closed circuit (DBD or direct contact) between electrode and notional treated surface, i.e. measurement equipment.

Optical emission spectroscopy

The emission spectrum of the electrode's glow discharge was recorded using an AvaSpec-3648 Fiber Optic Spectrometer (Avantes, Apeldoorn, The Netherlands) with 10-μm slit and wavelength range 200–1100 nm, lens of which was placed at the distance of 60 mm from the plasma electrode. Maximum output intensity (100%) was chosen in the menu of Ozonix device. AvaLight-DH-CAL source was used to calibrate for absolute spectral intensity in the range 200–1099 nm. Time of signal integration in all the measurements was 500 ms. Data acquisition was done by AvaSoft-All software package. The NIST data base was used for the identification of atomic spectral lines and spectral simulation of spectra [30].

Electric field measurement

The oscilloscope used for the measurement of electric field strength, generated by the glow discharge of the plasma electrode, was WaveRunner 640Zi (Teledyne LeCroy Inc., CA, USA), the input impedance of which is 1 MΩ || 14 pF. A 16-mm-long monopole antenna (wire AWG 16) was installed via a BNC connector on a ground plane (1.6 mm thick FR-4 glass epoxy panel laminated with copper layer on both sides, 1 m × 1 m in size). Antenna and ground plane were connected to the oscilloscope and the patient grounding electrode of Ozonix device was connected to the ground plane. The applicator with the electrode was mounted on the antistatic expanded polystyrene holder which allowed precise positioning of plasma electrode in relation to antenna. In order to eliminate the influence of measurement equipment on the electric field of the electrode as well as to protect sensitive electronics of the oscilloscope, the distance of 10 mm between the antenna and plasma electrode (in which no DBD can occur) was determined as the closest "safe" distance at which measurements were conducted. The measured data were used for extrapolation of electric filed strength in the close proximity of the plasma electrode's surface (below 10 mm).

In all the measurements, the distance between the ground plane and the lowest point of the lens-shaped part of the plasma electrode was 10 mm. The distance between lens-shaped surface of the electrode and the antenna was changed in steps of 10 mm for interval from 10 mm up to 100 mm. At each distance between the antenna and lens-shaped surface of the electrode voltage waveforms were recorded for 10 different output intensities (10%–100% in steps of 10%) and the data were processed and analysed by MATLAB R2015b (MathWorks, Natick, MA, USA).

The relationship between the electric field strength (E) and induced open-circuit voltage (U_{oc}), measured on the terminals of a dipole antenna (as a monopole antenna, over a perfect conductive surface, has the same radiation pattern as a dipole antenna), is given by [31]

$$E = \frac{4U_{oc}[2\mathrm{In}(\iota a^{-1}) - 2 - \mathrm{In}4]}{\iota[2\,\mathrm{In}(\iota a^{-1}) - 1]} \quad (1)$$

where, l is the physical length of dipole antenna a is its radius. For l = 32 mm and a = 0.6554 mm, characteristic for the used antenna (1) can be reduced to

$$E = \frac{U_{oc}}{0.0123} \quad (2)$$

The electric field strength (E) is expressed in V/m.

Results and discussion

Emission spectrum analysis

Plasma electrode's glow discharge emission spectrum was recorded at 60-mm distance from the lens-shaped part of the electrode (Figure 3).

Spectral lines recorded in the red and near-infrared (R-NIR) wavelength range from 540 to 886 nm are shown in Figure 3. In the region below 540 and above 886 nm, no spectral lines were recorded. The most expressive spectral lines are recorded at 585, 588, 594, 602, 607, 609, 614, 616, 626, 632, 633, 640, 650, 653, 659, 667, 671, 692, 705, 724, 743 and 837 nm. These lines were identified as the atomic lines of neutral neon (Ne I). The spectral lines recorded at 700, 777 and 844 nm can be ascribed to neutral oxygen atom (O I).

A spectral simulation of neon spectra showed electron excitation temperature between 0.5 and 0.75 eV and of oxygen spectra 0.25 eV, respectively. Properties of spectrum can be attributed to excitation and consequent relaxation of neon and oxygen atoms, which are present in the glow discharge of investigated plasma electrode. Dissociation energy of oxygen double bond is 5.15 eV whereas the lowest excitation energy of neon is 16.6 eV, which indicates relatively high energy of

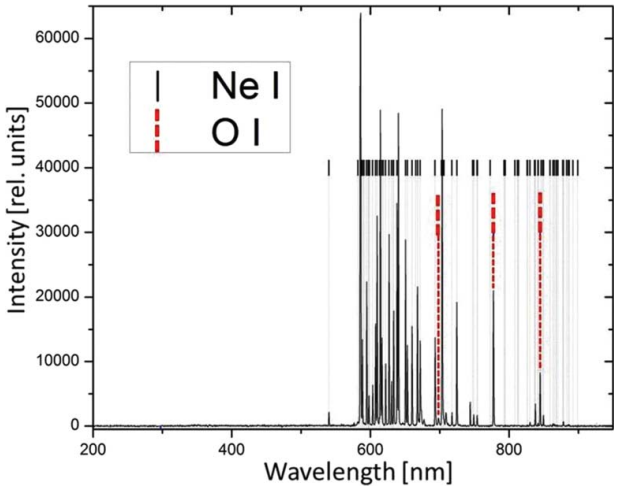

Figure 3. Emission spectrum of the plasma electrode's glow discharge in the range from 540 to 886 nm recorded at distance of 60 mm from the lens-shaped surface of the plasma electrode.

electrons which are present inside the glass chamber of plasma electrode [30].

It is reasonable to assume that the irradiance of recorded spectrum is additionally increased when plasma electrode is placed at the shorter distance from the treated surface, or when brought into direct contact with the treated surface. This assumption is evidenced by observed light scattering through translucent tissues during the clinical application of plasma electrode as well as increased brightness of the glow discharge in the case of closed circuit (DBD or direct contact) between the electrode and the treated surface (Figure 1).

Convissar [32], in his book, reported a wide spectrum of applications and positive results of photo-biomodulation in dental medicine. Numerous papers reported that irradiation with low-level R-NIR light (600–900 nm) shows wide variety of effects on tissues and on the cellular level, especially mitochondria and electron transport chain [33–36]. Karu [34] stated that a variety of diseases have definitively been demonstrated to depend on mitochondrial functions; this then makes it possible that the low-level light irradiation of mitochondria can affect their pathophysiological function.

Although mechanisms of photo-biomodulation are still not fully elucidated, most of the relevant studies indicate possible adsorption of light by the mitochondrial enzymes (especially wavelengths 613.5–623.5, 632.8, 667.5–683.7, 750.7–772.3 and 812.5–846.0 nm) [33–36]. Passarela and Karu [35] reported that irradiation with low-level monochromatic (laser) and narrow band (LED) light in specified spectrum can lead to stimulation of neuronal growth and of DNA and RNA synthesis; promotion of cell adhesion; improved neurological function; acceleration of wound healing; cellular and extracellular matrix proliferation; collagen production and granulation tissue formation; and reduction of the inflammatory response. With respect to the results of current study, it may be concluded that the emission spectrum of the plasma electrode coincides with the above-specified spectrum which shows bio-modulating properties.

Absorption of R-NIR spectrum may lead to local temperature increase; excitation of flavin and cytochrome in mitochondrial respiratory chain with consequent influence on transport of electrons; production of reactive oxygen species through excitation of endogenous porphyrins; and photo-activation of calcium channels with increase of intracellular calcium concentration and consequent cellular proliferation [34,36]. Reports regarding the application of R-NIR spectrum also indicate positive results in the early phase of wound healing of bone defects [37], osteogenic differentiation in mesenchymal stem cells [38] and dental pulp stem cells [39], as well as the improved bone healing and reduction of loading time of dental implants [40]. Therefore, it is reasonable to assume that R-NIR

spectrum emitted by the glow discharge of plasma electrode might have an important role in stimulation of regenerative processes, which is also evidenced by several clinical studies in which bone and soft tissue regeneration is reported [18–20].

Chen et al. [41] in their meta-analysis (14 reports) concluded that R-NIR light therapy did not significantly reduce pain but did significantly improved the functional outcomes of patients with temporomandibular disorders (TMDs). Panhoca et al. [42] showed that low-level R-NIR photo-stimulation can be useful in improving outcomes related to pain relief and mandibular range of motion for TMD patients, while de Castro et al. [43] reported reduction of inflammatory infiltrate in the TMJ. These effects could explain similar results reported by Doğan et al. [25] for extra-oral application of plasma electrodes in direct contact with the skin in projection of the underlying TMJ.

However, although wavelengths of the spectral lines emitted by the glow discharge of the plasma electrode correspond to the bioactive R-NIR wavelengths specified in a number of scientific papers, to validate the range of their biological effects and therapeutic value, it would be necessary to carry out further radiometric measurements which would determine power, radiant energy, radiant exposure and pulse parameters of the emitted spectrum.

Electric field analysis

Pulsed voltage waveforms (impulse frequency: 1053 Hz) were recorded in the treatment field. Impulses were characterized by the exponentially damped sine waveform in the range of 33 kHz (Figure 4).

The values of maximum amplitude voltage (U_{oc}) as a function of distance (from 10 to 100 mm) for all

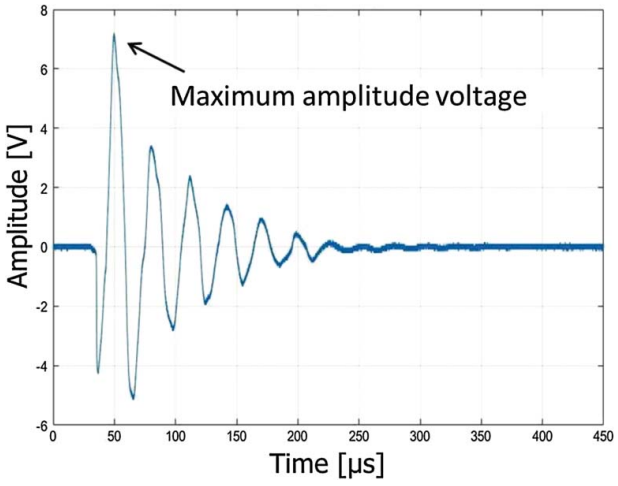

Figure 4. Voltage waveform recorded at 100% output intensity and 10-mm distance with pulse frequency 1053 Hz, exponentially damped sine wave in range of 33 kHz, pulse duration 200 μs – duty cycle 20%. Maximum amplitude voltage (arrow) was used for the calculation of the electric field strength.

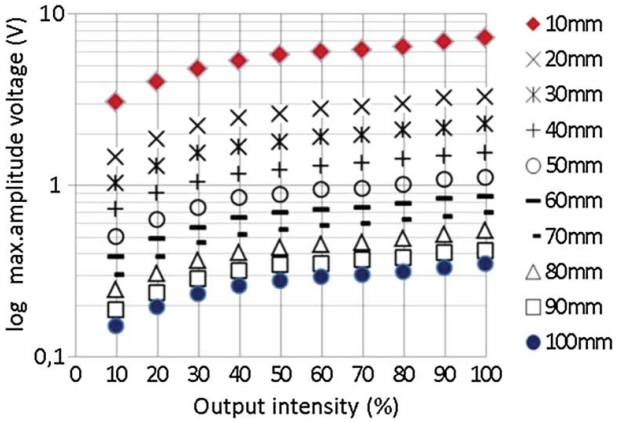

Figure 5. Maximum amplitude voltage (V) measured on monopole antenna with respect to distance (10–100 mm) and output intensity (10%–100%).

output intensities (10%–100% in steps of 10%) ranging from $X \pm SD = 0.27 \pm 0.06$ V (at 100 mm) to $X \pm SD = 5.56 \pm 1.29$ V (at 10 mm) were recorded (Figure 5).

Electric field strength values were calculated from maximum amplitude voltage values (2) for all intensities (10%–100%) and distances (10–100 mm) from the lens-shaped surface of the electrode (Appendix 1). At 100-mm distance from the electrode's surface, the electric field strength ranged from 12.44 V/m at 10% intensity to 28.46 V/m at 100% ($X \pm SD = 22.15 \pm 5.04$ V/m) and at 10-mm distance from 248.86 to 587.32 V/m ($X \pm SD = 451.69 \pm 105.13$ V/m), respectively (Figure 6).

The power function ($E = U/d^b$) showed the closest fitting to experimental results. Functions for maximum ($E = 13{,}702/d^{1{,}305}$, $R^2 = 0.9863$) and minimum ($E = 5855.8/d^{1{,}294}$, $R^2 = 0.9809$) output intensities, where $l\,d = 1$ mm (Figure 7). Functions were used to approximate the electric field strength in the close proximity (below 10 mm) to the plasma electrode's surface (Figure 8). In such way, estimated electric field strength was in the range from 5.8 to 13.7 kV/m at 1-mm distance and between 10^6 and 10^8 V/m in the close proximity of electrode's surface (below 0.01 mm).

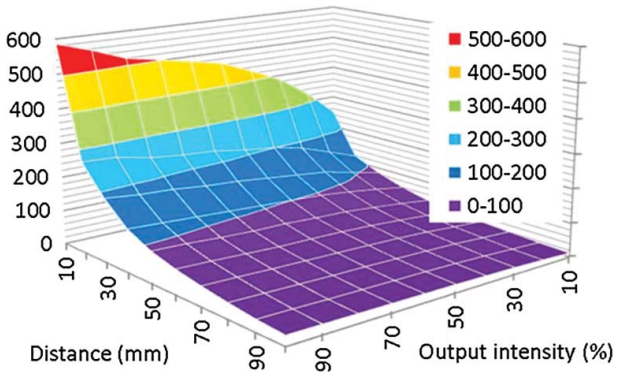

Figure 6. Electric field strength (V/m) increases with the increase of output intensity and with the reduction of distance although the reduction of distance shows higher impact (steep incline of the plane on the distance axis).

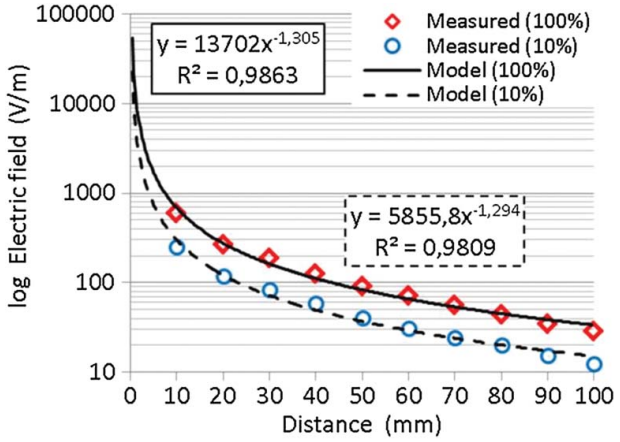

Figure 7. Power function ($E = U/d^b$) fitting the experimental results for minimum (10%) and maximum (100%) output intensity (shown in logarithmic scale).

The electric field in the air above the earth's surface is typically 100 V/m, but during strong electric storms, it may increase 10-fold or more [44]. Due to the insignificant transmission of low-intensity fields through air by radiation, such fields are usually applied through direct contact of the electrode and skin. Hence, we can assume that relatively low-intensity field applied at 10-mm distance from the treated surface probably has no significant biological effect.

However, the trend of increase of electric field strength with reduction of distance described by power function ($E = U/d^b$) and extrapolated values of the electric field strength indicate relatively high values of electric field in close proximity of the electrode (Figure 8). In such way, estimated values of electric field are in range from 10^6 to 10^8 V/m in the close proximity of electrode's surface (below 0.01 mm). Such approximation is in line with the electric field strength which is considered as precondition for achievement of electric breakdown in the air gap (3×10^6 V/m) [11].

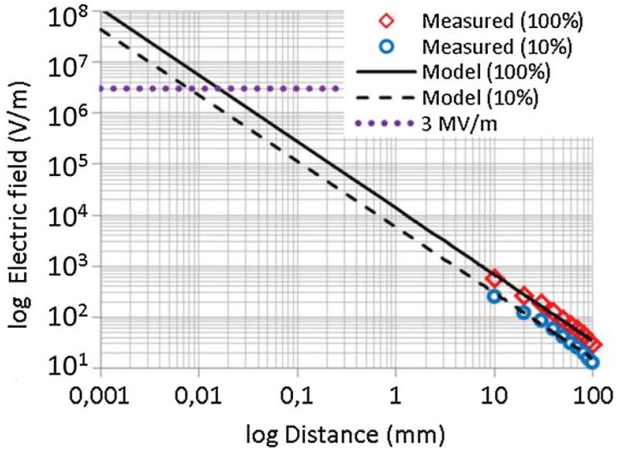

Figure 8. Estimated values of the electric field strength (V/m) for minimum and maximum output intensities predict a dielectric strength of air (3 MV/m) to be exceeded in the close proximity (<0.01 mm) electrode (show in logarithmic scale).

Constant U in proposed power function (Figure 5 (a)) also estimates the voltage of the plasma electrode ($U = E \times d^b$) to be in range from 5.8 kV (at 10% intensity) to 13.7 kV (at 100%) which can be related to the manufacturer's technical data (output voltage between 3 and 18 kV). According to *Paschen's law*, such derived values of electrode's voltage define the value of $p \times d$ (55–220 mmHg × cm) predicting the distance between the surface of the electrode and treated surface (at atmospheric pressure), at which electrical breakdown in air can occur, to be in the range <0.9 mm (at 10% intensity) to <3.1 mm (at 100%) [11]. These results are also in favour of clinical observations in which DBD indeed can be generated only below these distances depending on the chosen output intensity of the device.

Here it has to be emphasized that the estimated values of electric field only represent conditions in standby mode of the electrode. In the case of the closed circuit (DBD or direct contact) between plasma electrode and treated surface, the voltage and electric field of the electrode will certainly be significantly lowered due to the flow of the electric current.

Xiao [11] stated that the electric discharge in air gap, in addition to electric field strength and distance between electrodes, will depend on numerous other factors, e.g. the shape of the electrode, uniformity of the electric field and the voltage rise time. Therefore, numerous corrective factors are used in case of extrapolation of electric field strength in air gap discharges where additional complex physical mechanisms can cause fluctuations in electric field [45]. In such case both constants (U and b) in the proposed power function could be significantly altered. The values of the electric field strength in the case of direct contact of the plasma electrode and tissue or liquid will additionally be dependent on the current density and electric properties of the treated medium, e.g. resistivity, conductivity and/or impedance, as well as the applied frequency [46].

Although the primary function of the investigated system, according to manufacturer, is production of ozone by means of DBD, in the appropriate available literature, electric field generated by plasma electrode is not considered as an active component in the treatment field [16–25]. Medical appliances using low-to-moderate intensity radio-frequency electromagnetic fields (RF-EMF) in the range from 30 kHz to 300 MHz are commonly used in the treatment of bone fractures, wounds or pain, and oedema [44]. Kumaran and Watson [47,48], in their review articles (120 reports) on therapeutic effects of RF-EMF, listed numerous clinical studies reporting positive effects in reduction of pain, oedema, erythema, inflammatory processes, stimulation of healing and re-establishment of function, as well as reduced analgesic drug intake and reduced length of hospitalization. Al-Badavi et al. [49] also

reported application of pulsed radio-frequency (impulse frequency 600 Hz, pulse modulation 250 kHz) as safe and effective treatment for TMJ arthralgia and increasing mandibular range of motion. With respect to the recorded characteristics of the electric field, it can be assumed that certain therapeutic effects could be correlated with the interaction of the electric field and treated tissues. Therefore, this effects should be taken into consideration, especially in the line of explanation of therapeutic effects reported by several author s [17–19, 25], which could not be explained by topical bio-oxidative effects of ozone.

Biological effects of EMFs are ascribed to thermal and non-thermal mechanisms. Application of thermal effects of EMF may vary from mild (diathermy: <41 °C) to high (thermal ablation: from 46 to ≥110 °C) increase of tissue temperature [50]. Thermal impacts are dependent on a variety of EMF parameters, such as intensity, pulse shape and width, and the pulse sequence type [51]. Most of the therapeutic effects ascribed to mild increase of temperature involve increased metabolic activity and vasodilatation with increased perfusion of the treated tissue [52]. Thermal effects have indeed been recognized by Doğan et al. [25] who reported that during the application of plasma electrode, patients did not feel pain, although they felt a mild increase in temperature in the temporomandibular region. It can be assumed this effect could have been induced, by both, the absorption of R-NIR light as well as the thermal effects of the electric field. In this sense, the thermometric analysis of a treatment field would give valuable insight on the range of local thermal effects of such treatment.

The most detectable non-thermal mechanism of interaction of the EMF and tissues is the effect of cellular excitation by ion efflux (movement of calcium and other ions) through voltage gated ion channels sensitive to the oscillating electric fields [53]. Dysfunction of neuronal calcium signalling has been linked to neuro-inflammatory and neurodegenerative processes [54]. Calcium metabolism has also been recognized as an important factor involved in regenerative processes [55]. Therefore, a possibility to influence calcium metabolism by externally applied electric fields has important clinical implications. This mechanism could also explain healing and pain reduction effects recorded in application of plasma electrode [16–20,25]. This is especially the cases when plasma electrode was used extra-orally in direct contact with skin in the projection of underlying jaw or TMJ [17,25].

Due to the induced charge on its surface, a cell polarization and movement (dielectrophoresis) as well as formation of large aqueous pores (electroporation) may occur. Wang [53] stated that low values of electric field do not cause electroporation but with the increase of field strength or pulse duration, various effects may be observed, i.e. gene transfection (10^4 V/m and pulse duration 20 ms), drug delivery ($>10^5$ V/m,<10 μs) or bacterial decontamination (10^5 to $>10^6$ V/m in microsecond range). With respect to properties of the recorded pulsed electric field (especially due to exponentially damped sine waveform character shown in Figure 2), it would be reasonable to assume that it might induce a wide spectrum of non-thermal effects from cell polarization to bacteria decontamination. However, due to the complex physical phenomena which occur in treatment field in the case of closed circuit (DBD or direct contact) between plasma electrode and treated surface, the scope of exact biological implications remain unclear. Therefore, the results obtained in this investigation do not allow further interpretation as implementation of fluid and plasma dynamics as well as bio-impedance models would be necessary in order to understand this implication more accurately. In order to precisely determine therapeutic window and possible biological impacts of the recorded electric field on treated tissues, a further research is needed, which would quantify properties and define *in situ* dynamics of the electric currents, voltage drops, energy distribution and dissipation during closed-circuit modes.

Conclusion

The results of present study confirm that properties of the factors, recorded in the treatment field, can be correlated with mechanisms underlying photostimulation [34,35] and electrostimulation [56,57]. Hence, these mechanisms should be considered in order to fully explain therapeutic effects achieved through the application of plasma electrode, regardless of the modality of its application. It is reasonable to assume that the electric field and emission spectrum of a plasma electrode's glow discharge, as well as already recognized ozone and CAP, produce a cumulative effect on the treated tissue. The properties and therapeutic contribution of individual factors will most certainly depend on the mode of administration (electrode positioning, intensity and duration of exposure) as well as the properties of treated tissues. This is also evidenced by a broad spectrum of recorded clinical scores with respect to the different modes, sites and durations of application [14–26]. Possible therapeutic effects of electric field and R-NIR irradiation are especially substantiated by the reports in which it is not possible to explain obtained results through topical effects of gaseous ozone [17–19,25].

Complex conditions present in the treatment field, inability to isolate individual factors without compromising other factors in the treatment field, as well as similar therapeutic effects reported for each of its constituents [28,32,52] present a major challenge in terms of defining the appropriate model which would explain mechanisms underlying such therapeutic

procedure. Therefore, a more extensive multidisciplinary investigation is needed in order to evaluate physical properties and dynamics of these factors and elucidate exact mechanisms in which therapeutic effects are achieved.

Disclosure statement

No potential conflict of interest was reported by the authors.

References

[1] Crookes W. On radiant matter; a lecture delivered to the British Association for the Advancement of Science, at Sheffield, Friday, August 22, 1879. Am J Sci. 1879;18:241–262.

[2] Nehra V, Kumar A, Dwivedi H. Atmospheric non-thermal plasma sources. Int J Eng. 2008;2:53–68.

[3] Bittencourt JA. Fundamentals of plasma physics. New York (NY): Springer; 2004.

[4] Hoffmann C, Berganza C, Zhang J. Cold Atmospheric Plasma: methods of production and application in dentistry and oncology. Med Gas Res. 2013;3:21.

[5] Fridman A, Friedman G. Plasma medicine. Chichester (UK): John Wiley & Sons; 2012.

[6] Weltmann K-D, Polak M, Masur K. et al. Plasma processes and plasma sources in medicine. Contrib Plasma Phys. 2012;52:644–654.

[7] Daeschlein G, Napp M, von Podewils S. et al. Antimicrobial efficacy of a historical high-frequency plasma apparatus in comparison with 2 modern, cold atmospheric pressure plasma devices. Surg Innov. 2015;22:394–400.

[8] Napp J, Daeschlein G, Napp M. et al. On the history of plasma treatment and comparison of microbiostatic efficacy of a historical high-frequency plasma device with two modern devices. GMS Hyg Infect Control. 2015 (June 8); 10. doi:10.3205/dgkh000251.

[9] Strong FF. High frequency currents. New York: Remban Company; 1908.

[10] Kogelschatz U. Dielectric-barrier discharges: their history, discharge physics, and industrial applications. Plasma Chem Plasma Process. 2003;23:1–46.

[11] Xiao D. Dielectric strength of atmosphere air. In: Gas discharge and gas insulation. Berlin: Springer; 2016. p. 149–194.

[12] Chirokov A, Gutsol A, Fridman A. Atmospheric pressure plasma of dielectric barrier discharges. Pure Appl Chem. 2005;77:487–495.

[13] Prebeg D, Katunarić M, Budimir A. et al. Antimicrobial effect of ozone made by KP syringe of high-frequency ozon generator. Acta stomatol Croat. 2016;50(1):134–42.

[14] Tuncer D, Yazici AR, Ayturan S. et al. Antimicrobial effect of Ozone on cariogenic microorganisms in vitro. Ozone Sci Eng. 2013;35:456–464.

[15] Wilczynska-Borawska M, Leszczynska K, Nowosielski C. et al. Ozone in dentistry: microbiological effects of gas action depending on the method and the time of application using the ozonytron device. Experimental study. Ann Acad Med Stetin. 2011;57(2):99–103.

[16] Filipovic-Zore I, Divic Z, Duski R. et al. Impact of ozone on healing after alveolectomy of impacted lower third molars. Saudi Med J. 2011;32:642–644.

[17] Kazancioglu H, Kurklu E, Ezirganli S. Effects of ozone therapy on pain, swelling, and trismus following third molar surgery. Int J Oral Maxillof Surg. 2014;43:644–648.

[18] Kazancioglu HO, Ezirganli S, Aydin MS. Effects of laser and Ozone therapies on bone healing in the calvarial defects. J Craniof Surg. 2013;24:2141–2146.

[19] Ozdemir H, Toker H, Balcı H. et al. Effect of ozone therapy on autogenous bone graft healing in calvarial defects: a histologic and histometric study in rats. J Period Res. 2013;48:722–726.

[20] Tasdemir Z, Alkan BA, Albayrak H. The effects of Ozone therapy on the early healing period of de-epithelialized gingival grafts: a randomized placebo-controlled clinical trial. J Periodontol. 2016;1–17.

[21] Kazancioglu HO, Erisen M. Comparison of low-level laser therapy versus ozone therapy in the treatment of oral lichen planus. Ann Dermatol. 2015;27:485–o491.

[22] Pavelić B. Successful use of high frequency ozone generator and bio-oxidative therapy in endo-restorative treatment. 15th Biennial Congress of the European Society of Endodontology; 2011 Sept 15–17; Rome, Italy.

[23] Pavelić B, Katanec D, Šegović S. et al. Garres osteomyelitis resolved by endodontic treatment and use of ozone therapy: a case report. 14th Biennial Congress of European Society of Endodontology; 2009 Sept 23–26; Edinburgh, Scotland.

[24] Pavelić B, Plančak D. Application of biooxidative therapy in the treatment of periimplantitis. 4th International Congress of the Croatian Society of Dental Implantology of Croatian Medical Association; 2011 Oct 6–8; Opatija, Croatia.

[25] Dogan M, Özdemir Dogan D, Düger C. et al. Effects of high-frequency bio-oxidative ozone therapy in temporomandibular disorder-related pain. Med Prin Pract. 2014;23:507–510.

[26] Agrillo A, Filiaci F, Ramieri V. et al. Bisphosphonate-related osteonecrosis of the jaw (BRONJ): 5 year experience in the treatment of 131 cases with ozone therapy. Eur Rev Med Pharmacol Sci. 2012;16:1741–7.

[27] German I, Rodrigues A, Andreo J. et al. Ozone therapy in dentistry: a systematic review. Int J Odontostomatol. 2013;7:267–78.

[28] Graves DB. Low temperature plasma biomedicine: A tutorial review. Phys Plasmas (1994-present). 2014;21:080901.

[29] Erdemci F, Gunaydin Y, Sencimen M. et al. Histomorphometric evaluation of the effect of systemic and topical ozone on alveolar bone healing following tooth extraction in rats. Int J Oral Max Surg. 2014;43:777–783.

[30] Kramida A, Ralchenko Y, Reader J. NIST Atomic Spectra Database, version 5, National Institute of Standards and Technology, Gaithersburg, MD. (retrieved on August 15th 2015). 2015. Available from: http://www.nist.gov/pml/data/handbook/index.cfm.

[31] Stephan AD. Survey of instrumentation and measurement. New York: Wiley-IEEE; 2001.

[32] Convissar RA. Principles and practice of laser dentistry. St. Louis (MI): Elsevier Health Sciences; 2015.

[33] Karu T, Kolyakov S. Exact action spectra for cellular responses relevant to phototherapy. Photo Laser Therapy. 2005;23:355–361.

[34] Karu TI. Cellular mechanisms of photobiomodulation. In: de Freitas, Simões, editors. Lasers in dentistry: Guide for clinical practice. Oxford (UK): Wiley; 2015. p. 251–274.

[35] Passarella S, Karu T. Absorption of monochromatic and narrow band radiation in the visible and near IR by both mitochondrial and non-mitochondrial photoacceptors results in photobiomodulation. J Photochem Photobiol B Biol. 2014;140:344–358.
[36] Tafur J, Mills PJ. Low-intensity light therapy: Exploring the role of redox mechanisms. Photomed Laser Surg. 2008;26:323–328.
[37] Deniz E, Arslan A, Diker N. et al. Evaluation of light-emitting diode photobiomodulation on bone healing of rat calvarial defects. Biotech Biotechnol Equip. 2015;29:758–765.
[38] Kim HK, Kim JH, Abbas AA. et al. Red light of 647 nm enhances osteogenic differentiation in mesenchymal stem cells. Lasers Med Sci. 2009;24:214–222.
[39] Tabatabaei FS, Torshabi M, Nasab MM. et al. Effect of low-level diode laser on proliferation and osteogenic differentiation of dental pulp stem cells. Laser Phys. 2015;25:095602.
[40] Lopes CB, Pinheiro AL, Sathaiah S. et al. Infrared laser light reduces loading time of dental implants: a Raman spectroscopic study. Photo Laser Therapy. 2005;23:27–31.
[41] Chen J, Huang Z, Ge M. et al. Efficacy of low-level laser therapy in the treatment of TMDs: a meta-analysis of 14 randomised controlled trials. J Oral Rehab. 2015;42:291–299.
[42] Panhoca VH, de R, Lizarelli FZ. et al. Comparative clinical study of light analgesic effect on temporomandibular disorder (TMD) using red and infrared led therapy. Lasers Med Sci. 2015;30:815–822.
[43] de Castro IC, Rosa CB, Carvalho CM. et al. Assessment of different energy delivery settings in laser and LED phototherapies in the inflammatory process of rat's TMJ induced by carrageenan. Lasers Med Sci. 2015;30:2105–2113.
[44] Francisco A-C, del Mar S-AM, Irene C. et al. Could radiotherapy effectiveness be enhanced by electromagnetic field treatment?. Int J Mole Sci. 2013;14:14974–14995.
[45] Drummond JE. Plasma physics. Mineola (NY): Dover Publications; 2013.
[46] Faes T, Van der Meij H, De Munck J. et al. The electric resistivity of human tissues (100 Hz-10 MHz): a meta-analysis of review studies. Physiol Measure. 1999;20:R1.
[47] Kumaran B, Watson T. Radiofrequency-based treatment in therapy-related clinical practice–a narrative review. Part II: chronic conditions. Phys Therapy Rev. 2016;1–19.
[48] Kumaran B, Watson T. Radiofrequency-based treatment in therapy-related clinical practice-a narrative review. Part I: acute conditions. Phys Therapy Rev. 2015;20:241–54.
[49] Al-Badawi EA, Mehta N, Forgione AG. et al. Efficacy of pulsed radio frequency energy therapy in temporomandibular joint pain and dysfunction. CRANIO®. 2004;22:10–20.
[50] Kumar P, Kumar D, Rai K. A numerical study on dual-phase-lag model of bio-heat transfer during hyperthermia treatment. J Thermal Biol. 2015;49:98–105.
[51] Guo L, Kubat NJ, Isenberg RA. Pulsed radio frequency energy (PRFE) use in human medical applications. Electromag Biol Med. 2011;30:21–45.
[52] de Oliveira Guirro EC, de Jesus Guirro RR, Dibai-Filho AV. et al. Immediate effects of electrical stimulation, diathermy, and physical exercise on lower limb arterial blood flow in diabetic women with peripheral arterial disease: a randomized crossover trial. J Manipul Physiol Ther. 2015;38:195–202.
[53] Wang Z. Electromagnetic field interaction with biological tissues and cells [dissertation]. London (UK): Queen Mary University of London; 2009.
[54] Fairless R, Williams SK, Diem R. Dysfunction of neuronal calcium signalling in neuroinflammation and neurodegeneration. Cell Tissue Res. 2014;357:455–462.
[55] Lansdown AB. Calcium: a potential central regulator in wound healing in the skin. Wound Repair Regen. 2002;10:271–285.
[56] Foster KR. Thermal and nonthermal mechanisms of interaction of radio-frequency energy with biological systems. Plasma Sci IEEE Trans. 2000;28:15–23.
[57] Markov MS. Electromagnetic fields in biology and medicine. London (UK): Taylor and Francis CRC Press; 2015.

Appendix 1. Strength of the electric field (V/m) recorded for different output intensities (10%–100%) and distances (10–100 mm) from the lens-shaped surface of the plasma electrode.

	Intensity									
d (mm)	10%	20%	30%	40%	50%	60%	70%	80%	90%	100%
10	248	327	388	429	466	485	503	520	556	586
20	118	150	181	201	211	226	232	242	262	267
30	84	105	125	135	145	155	161	171	176	186
40	59	73	85	95	100	105	110	115	120	125
50	41	52	61	69	72	77	78	82	88	91
60	31	40	47	53	57	59	60	64	68	71
70	25	31	38	42	45	47	49	51	54	56
80	20	25	30	33	35	37	38	40	42	44
90	15	19	23	26	28	29	30	31	33	34
100	12	16	19	21	23	24	25	26	27	28